Response to Editor and Reviewer

Dear Editor and Reviewer,

First and foremost, we sincerely thank you for dedicating your valuable time to providing such rich, valuable, detailed, and highly constructive comments on our study (**Manuscript title**: Forest and bioenergy expansion amplifies climate warming by accelerating regional cloud loss; **Manuscript ID**: egusphere-2026-367). We were privileged to receive detailed and professional review comments from this expert; these insights further stimulated our study interest in the potential role of cloud cover in large-scale land use and cover change (LUCC) and prompted us to reflect on the climate impacts of highly popular afforestation initiatives. These valuable comments have undoubtedly significantly enhanced the scientific rigor of the manuscript, the readability of the figures, and the reliability of the conclusions. We would like to express our sincerest gratitude once again to the editors and reviewers for their valuable time and effort.

Now, we provide a comprehensive, point-by-point response to the specific comments raised by the reviewer.

Major comments

1. LUCC Maps: In the main text (e.g., Lines 192-197), different land-use simulations are described, but the spatial distribution of the LUCC forcing is relegated to the supplement (Fig. S23). Because the cloud response depends on the specific latitude bands and local background conditions (e.g., Duveiller et al. (2021), Xu et al. (2022)), understanding exactly where the afforestation and bioenergy expansion occur is critical to interpreting the paper's core findings. I strongly recommend moving the LUCC maps to the main text (perhaps as a new Fig. 1) and addressing two main limitations of the current Fig. S23. First, the terminology is inconsistent with the main text (e.g., is "ORI" essentially the "CTL" simulation?). Second, the figure plots absolute mean percentages rather than the difference relative to the control, which makes it visually challenging to identify where the land cover changes actually occur, particularly for the REAL

scenario (comparing panels 'a' and 'c'). Crucially, these maps should be replotted as difference maps from CTL using standardized terminology, so the reader can immediately identify the geographic locations and magnitude of the land cover forcing driving the cloud responses.

First and foremost, we sincerely appreciate the valuable time and effort you dedicated to helping us improve our study, and we are also very grateful for the issue you raised regarding improving the visualization of land use and land cover change (LUCC) maps. Indeed, as you mentioned, the response of cloud cover to large-scale LUCC depends heavily on the specific locations where land cover changes occur, because those specific locations often exhibit widely varying background climate, which happen to serve as the foundational conditions influencing how LUCC impacts cloud cover. Therefore, presenting the precise locations where changes in forest and bioenergy crops occur is critical for interpreting the cloud cover responses of interest in our study. To address this issue, we generated land use and land cover difference maps between the three sensitivity experiments (idealized afforestation AF50, idealized bioenergy expansion BE50, and realistic afforestation REAL) and the control experiment (CTL), as has indeed been standard practice in many previous studies, making such an improvement necessary. We still placed the newly drawn land use difference maps in the Supplementary Material rather than in the main text (this is because there are already enough figures in the main text, which are the most important ones retained after screening, whereas secondary figures or those used for auxiliary explanations were all placed in the Supplementary Information, and also to reduce the length of the main text). Regarding the land use difference maps, the new figure label is Figure S8; as for why it is not Figure S1, this is because prior to this, we also evaluated the simulation performance of the Community Earth System Model (CESM) for key atmospheric variables (cloud cover directly relevant to this study, temperature, and the newly added cloud cover trend comparison), which is a necessary step to ensure the accuracy of the CESM simulation results, whereas the land use simulation setup comes after the CESM simulation performance evaluation, so the land-use-related result figures were naturally placed further behind, which was also done to ensure that the figures appear in sequential order during the analysis of results in the main text. We also retained the original absolute land cover percentage maps (Figure S7) to intuitively view the geographic distribution of global forests or crops. Furthermore, we newly added Figure S9 to show the temporal changes in tree and bioenergy crop areas in the three sensitivity experiments relative to the control experiment (we simultaneously corrected ORI to CTL to avoid confusion); doing so allows readers to see more clearly how much tree area increased by the end of the 21st century relative to 2015 under the realistic afforestation scenario (approximately 7.5 million km^2), as well as how much tree area increased by the end of the 21st century under the idealized afforestation scenario (approximately 29 million km^2). While 29 million km^2 appears to be a large number, especially compared with the realistic afforestation scenario, previous studies have already shown that global grassland area is sufficient to support such idealized land-use conversion; more importantly, converting grassland or shrubland to forest aligns better with the Food and Agriculture Organization (FAO) definition of afforestation, namely a fundamental conversion of land type (e.g., from grassland to forest). Therefore, strictly speaking, our realistic afforestation sensitivity experiment does not qualify as afforestation. Such confusing usage of concepts is not uncommon, so categorizing it as forest enhancement or reforestation might actually be more appropriate, a point we also mentioned in the manuscript, but for formal consistency in the analysis of results, we still refer to it as afforestation.

We once again thank you for your valuable comments and please forgive our initial oversight. We initially thought that readers would be able to directly discern the areas of forest or bioenergy expansion through the maps of absolute percentages of forest or grassland, as such differences could be partially displayed through the shading of the color bar. However, to demonstrate the differences in land cover more intuitively, we decided to adopt your valuable suggestion and make improvements.

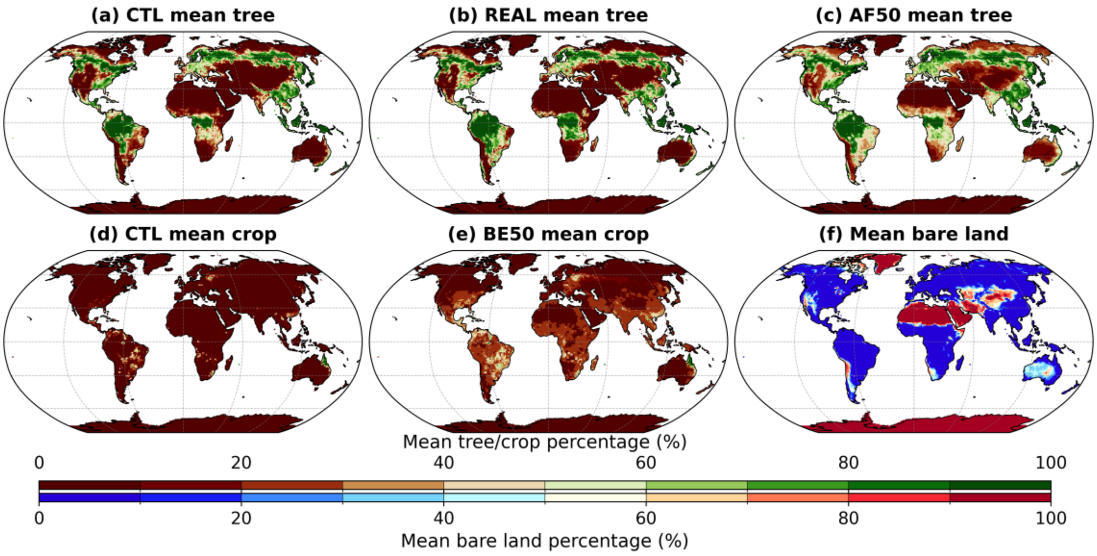

Figure S7. Spatial distribution of forest and bioenergy crop under different land use and land cover scenarios. (a and d) Spatial distribution of forests and bioenergy crops in the original land-use data (CTL run). (b) Spatial distribution of forests in the realistic afforestation scenario (REAL). (c and e) Spatial distribution of forests and bioenergy crops in the 50% idealized linear afforestation (AF50) and bioenergy crop expansion (BE50) scenarios. (f) Spatial distribution of bare land.

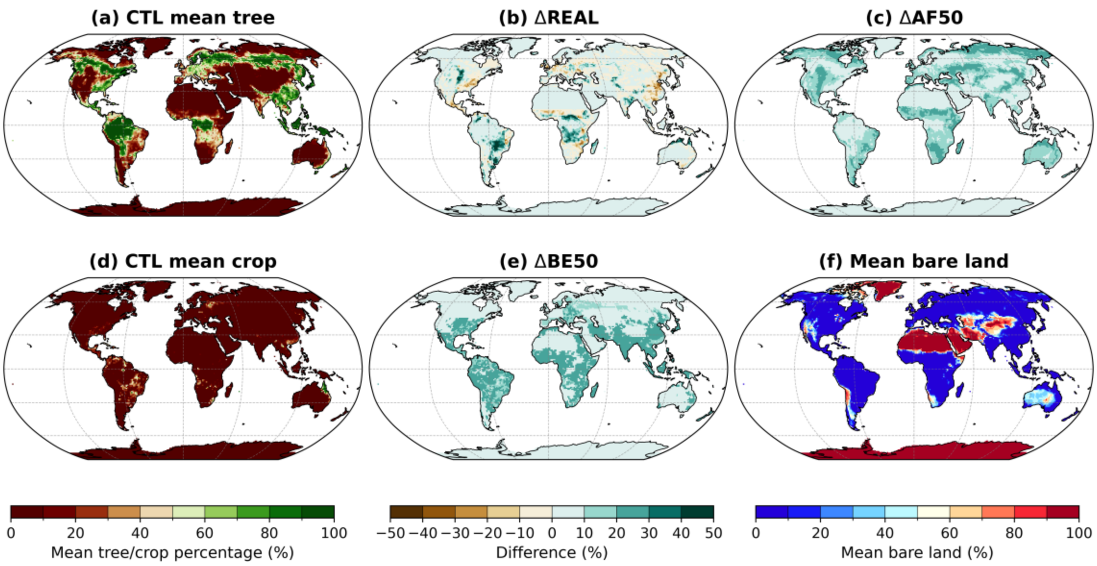

Figure S8. Spatial distribution of mean tree, crop, and bare land percentages and their differences under different land-use scenarios averaged over 2015-2100. (a and d) Mean tree and crop percentage in the CTL scenario. (b, c) Differences in tree percentage for the REAL and AF50 scenarios relative to CTL (ΔREAL and ΔAF50, respectively). (e) Difference in crop percentage for the BE50 scenario relative to CTL (ΔBE50). (f) Mean bare land percentage. The left and right color bars indicate the absolute percentages for vegetation (a, d) and bare land (f), respectively, whereas the middle diverging color bar represents the percentage differences between the forest and bioenergy expansion experiments and CTL scenario.

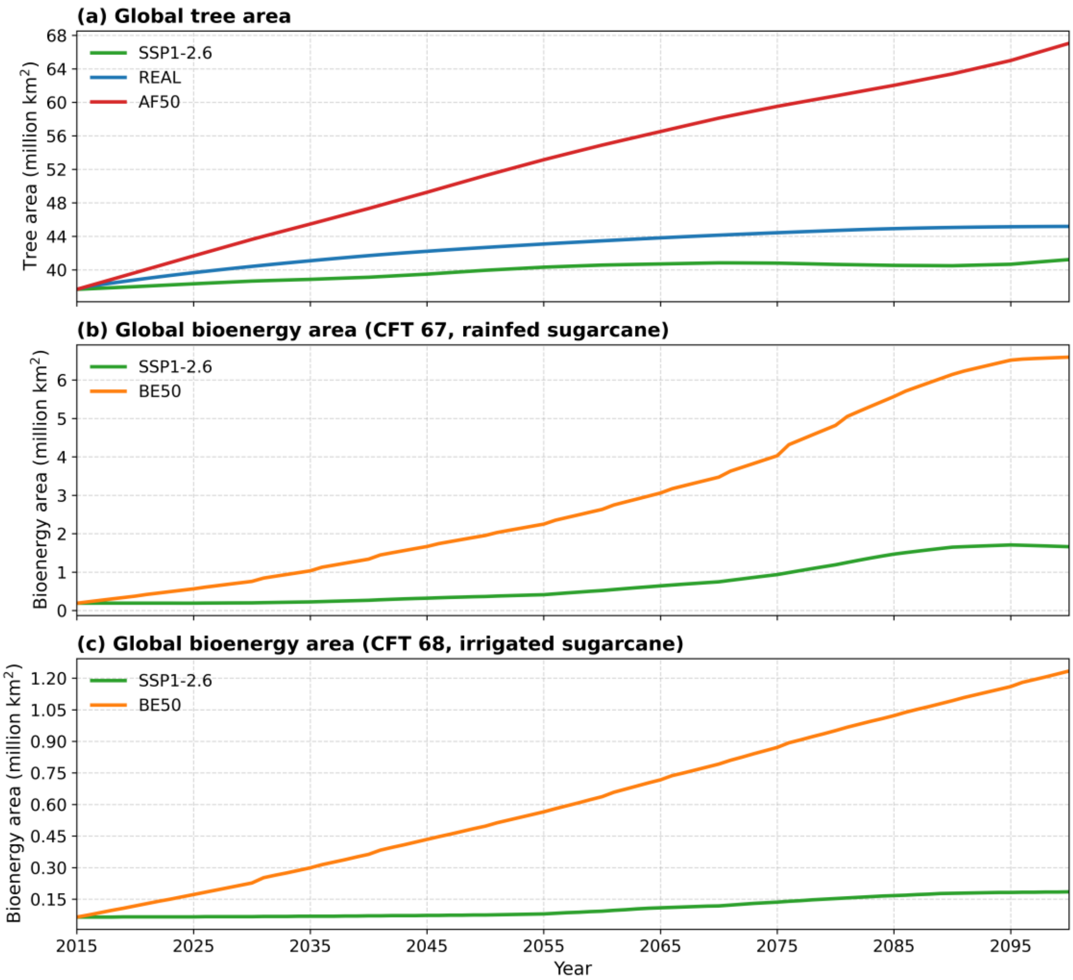

Figure S9. Area change of forest and bioenergy crops under different land-use scenarios (unit: million km2). In the Community Land Model Version 5 (CLM5), indices 67 and 68 correspond to rainfed and irrigated sugarcane, respectively, among bioenergy crops.

In CLM5, sugarcane is subdivided into rainfed sugarcane and irrigated sugarcane, with indices 67 and 68, respectively. Meanwhile, index 0 is bare ground; indices 1–8 are trees; and indices 9–14 are shrubs and grasslands, which are precisely the land sources for forest expansion in our study, conforming to the strict FAO definition of afforestation. In the bioenergy crop expansion simulation experiment, the land for sugarcane (rainfed and irrigated sugarcane) expansion originated from the land of remaining crops, as demonstrated by other researchers (https://github.com/AnushaNTNU/BetZy-scripts/blob/main/compare_modifiedvsoriginal_landuse.ipynb), which represents a trade-off state to ensure area conservation. Just as the land used in idealized afforestation comes from grasslands or shrublands, which is likewise to ensure area conservation, CESM strictly requires that land type modifications at the sub-grid level (patch-level) must ultimately sum to 100% at the grid level (grid-level).

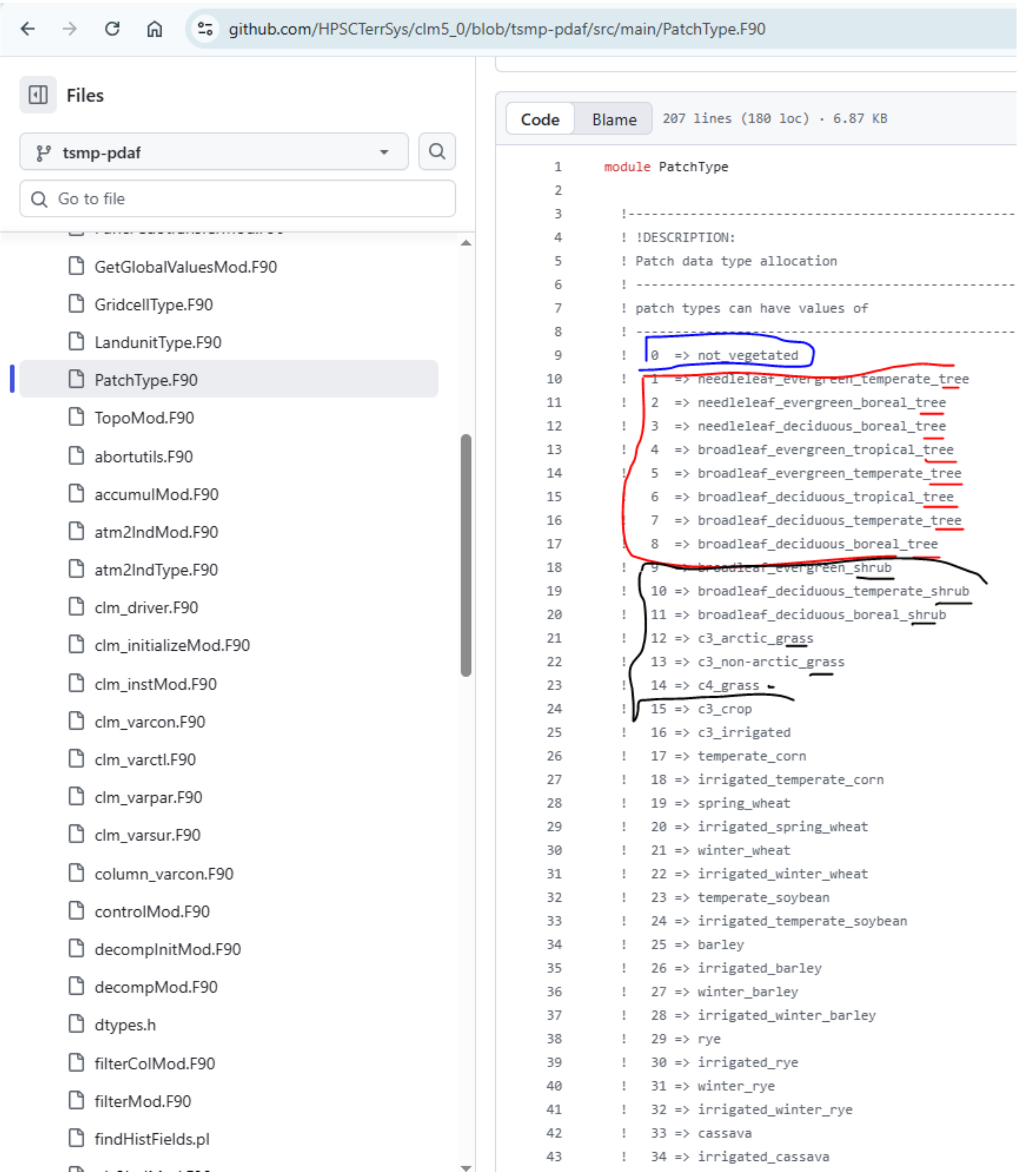

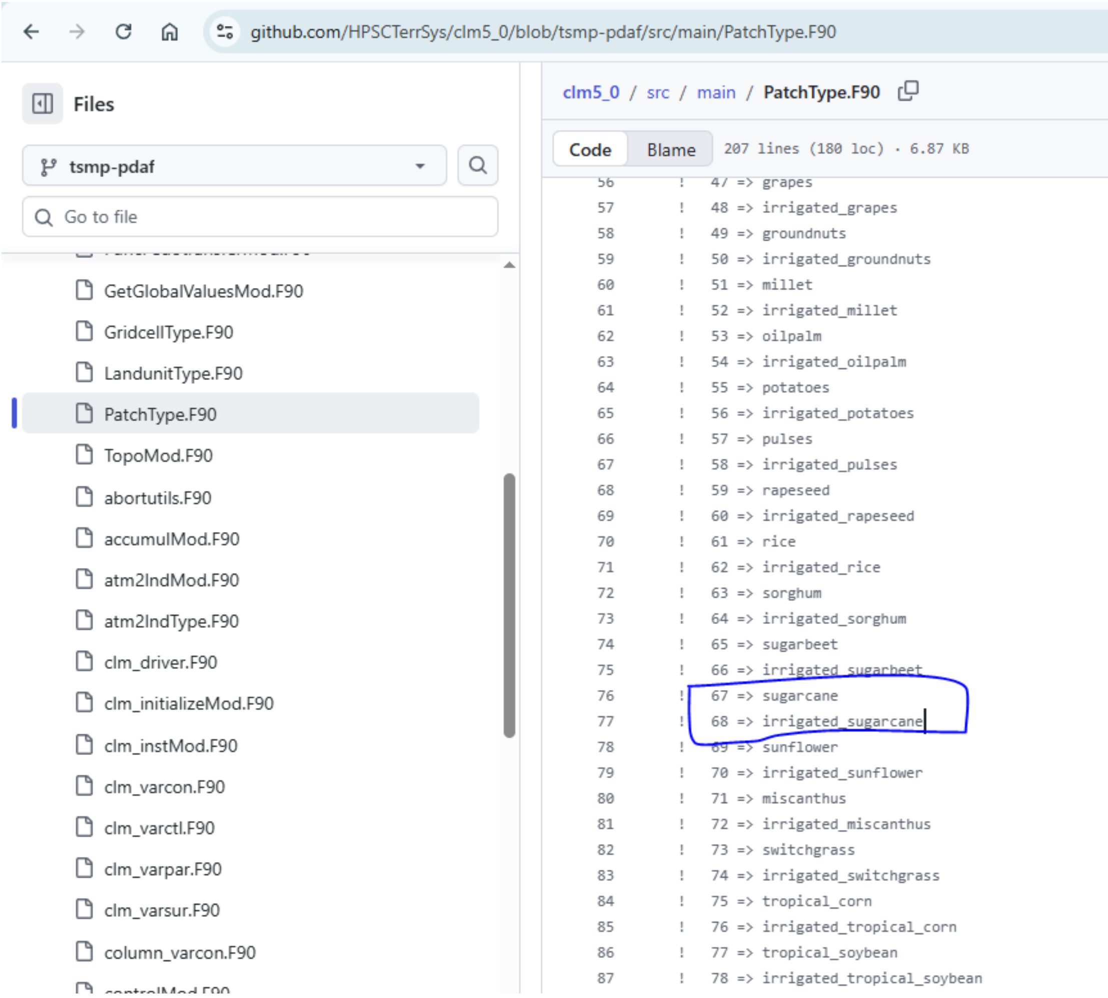

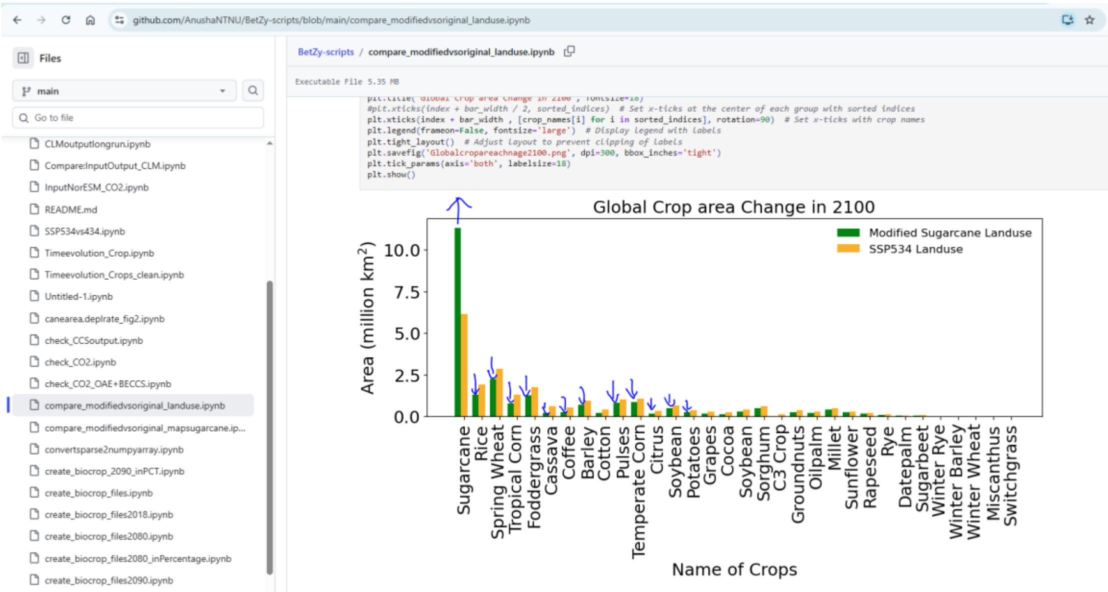

2. <u>Building on the previous comment regarding the LUCC maps, The authors claim in Line 442 that the high Gini index is "...suggesting amplified local land use impacts." Without showing where the LUCC forcing actually occurred relative to</u>

these trends, a "local" interpretation remains speculative. To my understanding, highly concentrated cloud trends do not necessarily indicate local forcing; they could equally be driven by non-local effects. More generally, utilizing a fully coupled model like CESM provides an excellent opportunity to account for both local and non-local LUCC effects, but this capability is underutilized in the current analysis. To address this, the authors should explicitly map the LUCC forcing areas and physically link them to the cloud trends to clearly differentiate local impacts from large-scale dynamical responses.

We are very grateful for the analysis you provided regarding leveraging CESM fully coupled simulations to gain insight into the local and non-local effects of climate responses to large-scale LUCC; we believe this is important, and this is also the core that distinguishes it from observational analyses, which lack exploration of non-local effects (observational analyses often employ space-for-time substitution methods to analyze the difference between a certain grid cell and surrounding grid cells to represent climate responses, thus rendering them powerless to evaluate non-local effects). In response to the first valuable suggestion, we explicitly added new maps to represent the differences in land use change across temporal and spatial scales. Then, regarding the issue of distinguishing local and non-local long-term cloud cover trends in response to large-scale LUCC, it may not be possible to decompose them into direct (local) and indirect (non-local) physical terms like decomposing surface temperature changes based on the surface energy balance (SEB) decomposition equation; at least at present, we have failed to find a similar method to decompose changes in cloud cover into local and non-local responses. In fact, in SEB, cloud feedback is already a non-local effect (as the SEB formula in the main text demonstrates, the meaning expressed by indirect is exactly non-local). However, we still have not currently discovered a suitable method directly applicable for decomposing cloud cover, which might be developed in future studies just like decomposing surface temperature into physical processes such as albedo, turbulent fluxes, and atmospheric feedbacks; therefore, to a large extent, what we can do currently is only to complete this part of the analysis by plotting land cover difference maps, but we chose to deepen the non-local effects of cloud cover in the discussion, especially why large-scale forest and bioenergy expansion occurs in terrestrial regions, yet changes also occur over the ocean. Obviously, the setup of a fully coupled model is merely the basic tool to explain this phenomenon, and this content has been placed in the discussion section. In addition, we added an analysis of temperature advection; this is because temperature is one of the key factors affecting cloud cover, and by analyzing temperature advection, we can know where the temperature increases are caused by remote temperature advection, thereby illustrating the non-local response of cloud cover. Regarding the spatial concentration of LUCC-induced cloud cover trends, we can observe it through the newly drawn land cover difference maps. Specifically, in the control experiment, the Gini index for the decreasing trend in total cloud cover in the Northern Hemisphere is 0.36, whereas it increased to 0.44 in the large-scale idealized afforestation experiment; similarly, the Gini index for low-level cloud loss in the Northern Hemisphere in the control experiment is 0.41, whereas it increased even further to 0.50 in idealized afforestation. As mentioned in the main text, a Gini index closer to 1 indicates greater inequality, signifying that fewer latitudinal bands contributed to a stronger cloud cover loss trend. The two sets of sharply contrasting data directly indicate the spatial aggregation of total cloud cover and low-level cloud losses in the Northern Hemisphere; when compared with the land cover maps of idealized afforestation, it can be found that these are precisely the regions of large-scale conversion from grassland or shrubland to forest.

We once again deeply thank you for your scientific insights into the non-local effects of cloud cover, which is indeed something we had not thought of previously; we never thought that cloud cover could also be decomposed into different physical processes like surface temperature changes. We believe that the issue of decomposing changes in cloud amount into local and non-local driving factors is full of scientific value, and we may maintain further investigation in future research, rather than merely analyzing it indirectly through methods such as temperature advection.

3. <u>Ambiguous Trend Reporting: The discussion of cloud-cover trends (Lines 298–</u>

336) is difficult to follow. For example, the use of "respectively" in Line 303 when describing CLDTOT trends is ambiguous, making it unclear how the AF50 and REAL simulations compare with CTL and BE50. Furthermore, expressions like "1.14 times increase in loss rate" and "1.52 times" are confusing. I suggest reporting straightforward percentage changes and/or the actual trend values for each experiment.

We are very grateful for your valuable comments. We have decided to check the full text to resolve similar issues, and adopt the valuable suggestion you provided where necessary, namely, directly providing specific percentage changes or actual trend values. However, in some places, we will still choose to provide multiples; doing so is to intuitively compare the intensity of the changes in cloud cover trends.

4. High-Cloud Response Clarification: The discussion of the high-cloud response (Lines 326–332) requires significant clarification. The manuscript argues that afforestation amplifies the positive trend in CLDHGH, enhancing climate warming. However, it is unclear which cloud populations contribute to this diagnostic. Line 161 states that the classification is based on cloud-top pressure thresholds. Is the classification based solely on cloud-top pressure/height? If so, deep convective clouds (rooted in the boundary layer) extending aloft could be classified as high clouds alongside thin cirrus. Because deep convection could respond to surface fluxes while cirrus may not do so directly, the physical mechanism linking LUCC to CLDHGH is ambiguous. Please clarify how CESM defines these cloud types and provide targeted mechanistic support for the high-cloud response.

We sincerely thank you for this highly insightful comment, which astutely points out a subtle nuance in the representation of cloud cover types in climate models. We completely agree that distinguishing between isolated cirrus clouds and deep convective clouds is crucial for establishing robust mechanistic connections. As you mentioned, the response of high-level clouds to large-scale land-use change was not clearly explained in our manuscript, particularly the fact that the positive response of high-level clouds is opposite to the negative response of low- and mid-level clouds. This contrasting response may stem from the fact that large-scale land-use change exerts a predominantly greater impact on low- and mid-level clouds (King et al., 2024: King, J. A., Weber, J., Lawrence, P., Roe, S., Swann, A. L. S., and Val Martin, M.: Global and regional hydrological impacts of global forest expansion, Biogeosciences, 21, 3883 – 3902, https://doi.org/10.5194/bg-21-3883-2024, 2024). In CESM, high-level cloud fraction (CLDHGH) is diagnostically defined as the vertically integrated cloud fraction strictly located above the 400 hPa pressure level, meaning that different cloud types are classified based on cloud-top pressure (https://github.com/ESCOMP/CAM/blob/14ad2a03080e727e45e2e1c18f865a90f28a76e1/src/physics/cam/cloud_cover_diags.F90). However, this classification purely based on cloud-top pressure means that CLDHGH inherently encompasses both in situ generated thin cirrus clouds and the high-altitude portions of deep convective clouds rooted in the boundary layer (e.g., convective cloud tops and detrained anvil clouds). Although isolated cirrus clouds may not directly respond to surface fluxes, deep convection undoubtedly does. Our machine learning attribution framework identified atmospheric water vapor and precipitation as the primary drivers of the LUCC-induced long-term trends in CLDHGH, indicating that the physical mechanisms linking LUCC to the high-level cloud response are intrinsically tied to these deep convective processes. Specifically, idealized afforestation fundamentally alters surface energy partitioning, moderately increasing local surface temperatures and moisture supply. This enhanced surface buoyancy forcing destabilizes the boundary layer, triggering more intense deep convective updrafts, which can be observed in the enhanced trends of convective available potential energy (CAPE). These changes induced by large-scale idealized afforestation transport excess water vapor from the boundary layer to the upper troposphere. Upon reaching altitudes above 400 hPa (particularly around 200 hPa), the subsequent detrainment of this water vapor, coupled with local cooling and increased relative humidity, collectively catalyzes the formation and extensive horizontal expansion of high-level clouds. This phenomenon is evident in both the idealized and realistic afforestation scenarios, whereas it is weaker in the bioenergy expansion experiment. This indirectly confirms that bioenergy expansion struggles to trigger the intense tropospheric atmospheric perturbations characteristic of forest expansion.

Therefore, the increasing trend in CLDHGH observed in our study is, in fact, a secondary dynamical consequence arising from the direct response of boundary layer convection to LUCC-driven surface flux anomalies. The increasing trend in high-level clouds and the decreasing trend in low- and mid-level clouds synergistically accelerate warming. Although their respective trends are in opposite directions, this indicates that large-scale idealized afforestation does not accelerate warming solely through the accelerated loss of low- and mid-level clouds. Notably, even realistic afforestation enhances the trend in high-level clouds, implying that even carefully planned realistic afforestation could generate positive radiative forcing at the top of the atmosphere. This contrasts starkly with the lower atmosphere and emphasizes that future research must adopt a whole-atmosphere perspective.

https://bg.copernicus.org/articles/21/3883/2024/

Global and regional hydrological impacts of global forest expansion
James A. King et al.

In our results, we find significant increases in low cloud fraction over Argentina in Base relative to No LULCC in 2095. In Max Forest, there are small but significant increases (~ 5 %) in low-level cloud fraction (below 700 hPa) over the Congo Basin, northern Australia, Uruguay, and Colombia and Venezuela in 2095 (Fig. 5a) with smaller yet significant increases of the same spatial pattern in 2050. All of these are areas with significant increases in tree cover in Max Forest. Significant differences in oceanic low cloud of both positive and negative signs are seen in both scenarios relative to No LULCC (Fig. 5a). However, given the moderate nature of our land use change scenarios, attributing these changes directly to forestation is challenging. While low cloud cover is important for the surface radiation balance, changes to deep convective clouds over the tropical rainforest basins can have important consequences for regional and global climate. We find statistically significant but small (~ 0.2 %) increases in tropical convective cloud fraction over Africa in Max Forest relative to No LULCC in 2095 (Fig. 5b), but the significant differences are restricted to below 900 hPa, implying a limited effect of the land use change scenario on deep convection.

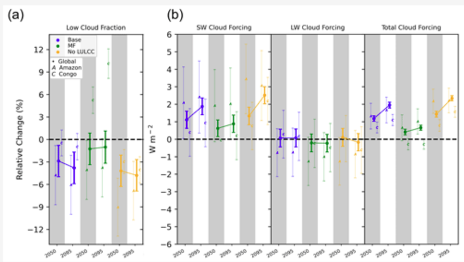

Figure 7 As Fig. 2b but showing differences in cloud cover integrated between 1200–700 hPa **(a)** and differences in clean-sky shortwave cloud radiative forcing, clean-sky longwave cloud radiative forcing, and total clean-sky cloud radiative forcing **(b)**.

github.com/ESCOMP/CAM/blob/14ad2a03080e727e45e2e1c18f865a90f28a76e1/src/physics/cam/cloud_cover_diags.F90

Files

14ad2a0

Go to file T

- aoa_tracers.F90
- beljaars_drag.F90
- beljaars_drag_cam.F90
- boundarydata.F90
- cam_diagnostics.F90
- cam_snapshot.F90
- carma_diags_mod.F90
- carma_flags_mod.F90
- carma_intr.F90
- carma_model_flags_mod.F90
- check_energy.F90
- chem_surfvals.F90
- cldfrc2m.F90
- cldwat2m_macro.F90
- cloud_cover_diags.F90
- cloud_diagnostics.F90
- cloud_fraction.F90

Code Blame 201 lines (168 loc) · 7.71 KB

```
!===============================================================================
! cloud cover output
!===============================================================================
module cloud_cover_diags

  use shr_kind_mod,  only: r8=>shr_kind_r8, shr_kind_CS
  use ppgrid,        only: pcols, pver,pverp
  use cam_history,   only: addfld, add_default, outfld, horiz_only
  use phys_control,  only: phys_getopts

  implicit none

  private

  public :: cloud_cover_diags_init
  public :: cloud_cover_diags_out

   real(r8) plowmax            ! Max prs for low cloud cover range
   real(r8) plowmin            ! Min prs for low cloud cover range
   real(r8) pmedmax            ! Max prs for mid cloud cover range
   real(r8) pmedmin            ! Min prs for mid cloud cover range
   real(r8) phghmax            ! Max prs for hgh cloud cover range
   real(r8) phghmin            ! Min prs for hgh cloud cover range
!
   parameter (plowmax = 120000._r8,plowmin = 70000._r8, &
              pmedmax =  70000._r8,pmedmin = 40000._r8, &
              phghmax =  40000._r8,phghmin =  5000._r8)


contains

```

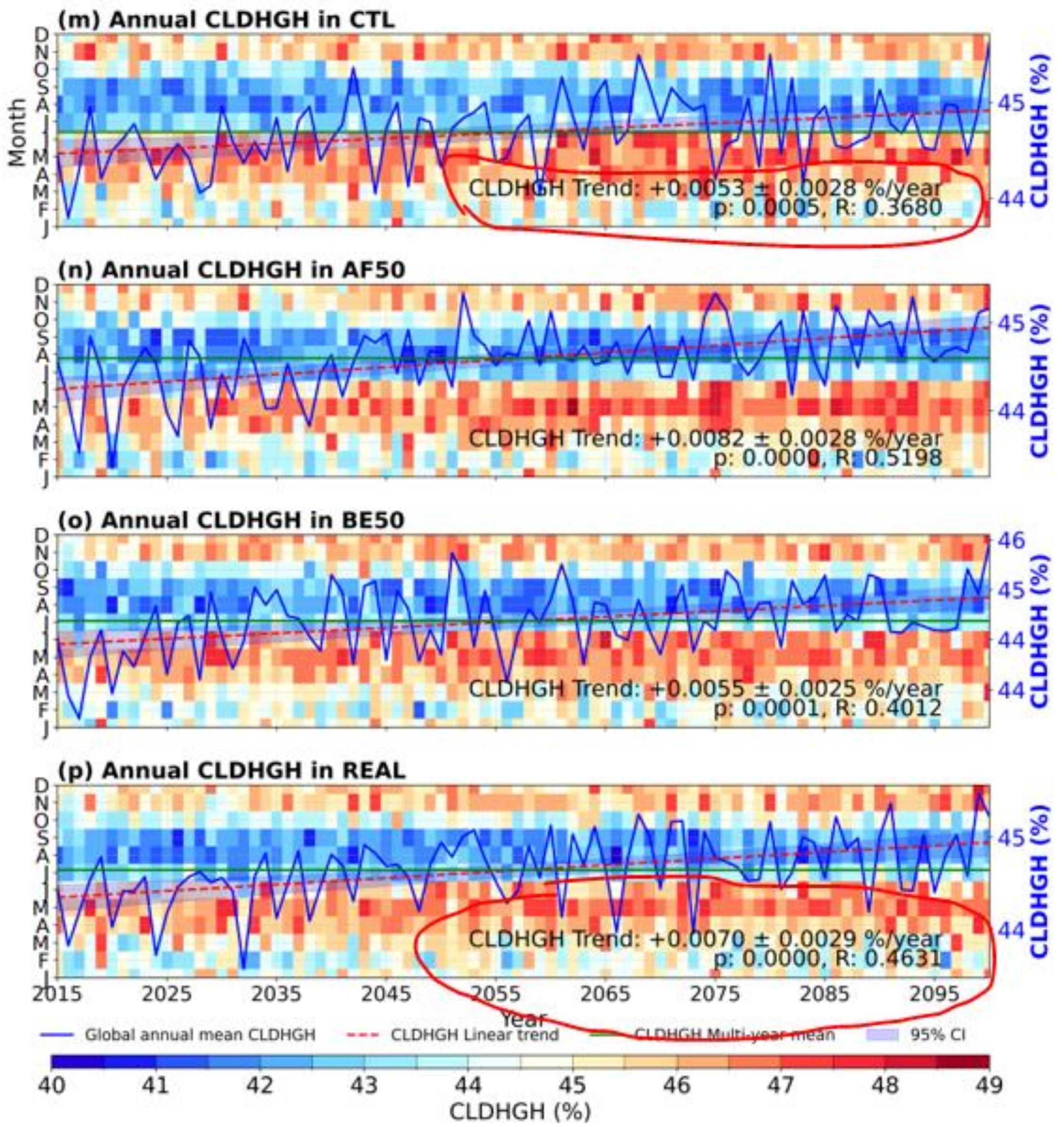

5. <u>Significance and Uncertainty: A discussion of statistical significance and model uncertainty is largely missing from the core results and should be included to validate the claimed trends.</u>

We are very grateful for your valuable comments, and we fully agree with conducting an objective discussion on the uncertainties in the presented research results. Particularly in Fig. 1, when calculating global mean trends, the uncertainty range was relatively large; however, when computing the land and ocean regions separately, the uncertainty narrowed significantly (Fig. S10). Upon inspection, this issue was caused by an error in the calculation code, which is addressed in our response to Comment 6.1.

On the other hand, in the discussion section, we further elaborated on the parametric uncertainties inherent in cloud parameterization within CAM6, the atmospheric component of CESM, as well as the limitations of our single-model experimental design. Regarding the machine learning driver attribution analysis, we strictly constrained the XGBoost model through 100 Bayesian hyperparameter optimization iterations to prevent overfitting, thereby rigorously mitigating uncertainties associated with machine learning; thus, the parameters presented in Table S1 represent the optimal parameter set. We deeply appreciate your kind reminder, as these additions regarding uncertainties and limitations have clearly substantially enhanced the rigor of our study.

6.1. <u>Figure Presentation and Interpretability: Figure 1： The shading representing the uncertainty is almost invisible, and the ± error bounds listed in the legend are massive (please see my separate major comment regarding the missing discussion on uncertainty). Furthermore, the text for the p-values and R-values is unreadable in several panels (e.g., Fig. 1n). Finally, the caption fails to explain what the different curves represent physically.</u>

We highly appreciate the reviewer's valuable comments. The issues raised regarding the excessively large uncertainty and the visual presentation in Fig. 1 are crucial for clarifying the underlying reasons and improving the figures. Furthermore, concerning the issue of where text labels in subfigures (such as Fig. 1n) were unclear or obscured, we have redrawn the figures and adjusted the positions of the text annotations to prevent any overlap. Initially, we considered placing the text inside a rectangular box with a white background; however, this approach risked obscuring the underlying heatmap. Therefore, we chose to reposition the text annotations to display them as clearly as possible. Additionally, we have included legends to explain the physical meanings of the different curves, and similar improvements have been applied to all subsequent figures.

Regarding the problem of the excessively wide confidence interval in Fig. 1, we reviewed the previous old calculation code and identified a computational error that led to this issue. In the old code, the lower and upper bounds returned by the user-defined function *calc_bootstrap_ci* represented the fluctuation range of the Y-values (absolute cloud fraction in %) corresponding to the entire fitted regression line for each year. Moreover, the step *ci_half=(ci_upper-ci_lower)[0]/2* mistakenly extracted the uncertainty of the global cloud baseline at the very first timestamp of the sequence (year in 2015). Consequently, it addressed the uncertainty interval of the global mean cloud fraction specifically for the year 2015. In the revised new code, percentiles are calculated directly from the distribution of the regression slopes obtained through 1000 bootstrap resamples via *slope_lower* and *slope_upper*. Thus, it correctly addresses the uncertainty interval of the rate of change in cloud fraction over the simulated 85-year period (2015–2100). In the revised manuscript, we have corrected this statistical method. We now explicitly extract the 95% confidence interval directly from the distribution of the bootstrapped regression slopes. The updated trend ensures strict dimensional alignment and an accurate representation of the trend's statistical significance. The text and corresponding figures have been revised accordingly. Additionally, we have checked the code used to calculate the trends separated by land and ocean (Fig. S10), and confirmed that this section contains no errors.

To evaluate the performance of CESM in simulating cloud cover trends, we have added a spatial trend comparison plot (Fig. S3) to the previously generated difference plots (Figs. S1 and S2). Since trends are the primary focus of this study, visualizing trend comparisons allows for a more direct illustration of the uncertainties in the simulation results. Fig. S3 reveals that the CESM-simulated trends for total cloud cover and low-level clouds show good overall agreement with reanalysis data over land areas, specifically indicating a widespread decrease at comparable rates. This comparison reinforces our confidence in the cloud cover simulated by CESM.

OLD

```python
import xarray as xr
import matplotlib.pyplot as plt
import numpy as np
import scipy.stats as stats
import cmaps
import matplotlib.ticker as mticker
from matplotlib.colors import BoundaryNorm
from matplotlib.lines import Line2D
import matplotlib.patches as mpatches

# ====================== 1. Trend calc ======================
def calculate_trends(data):
    years = np.arange(len(data))
    slope, intercept, r_value, p_value, std_err = stats.linregress(years, data)
    return slope, intercept, r_value, p_value

# ====================== 2. Bootstrap 95% CI ======================
def calc_bootstrap_ci(years, data, n_boot=1000, ci=95):
    x = np.arange(len(years))
    slope, intercept, _, _, _ = stats.linregress(x, data)
    fitted = intercept + slope * x
    resid = data - fitted

    boot_slopes = []
    boot_intercepts = []
    rng = np.random.default_rng()
    for _ in range(n_boot):
        boot_resid = rng.choice(resid, size=len(resid), replace=True)
        boot_y = fitted + boot_resid
        s, i, _, _, _ = stats.linregress(x, boot_y)
        boot_slopes.append(s)
        boot_intercepts.append(i)


    boot_slopes = np.array(boot_slopes)[:, np.newaxis]          # (n_boot, 1)
    boot_intercepts = np.array(boot_intercepts)[:, np.newaxis]  # (n_boot, 1)
    boot_trends = boot_slopes * x + boot_intercepts            # (n_boot, n_years)
    # -------------------------------

    lower = np.percentile(boot_trends, (100 - ci) / 2, axis=0)
    upper = np.percentile(boot_trends, 100 - (100 - ci) / 2, axis=0)
    return lower, upper

# ====================== 3. File path ======================
base_path_cldtot = 'C:/JupyterXPC/Cloud_Analysis_AF_BE_Cloud_Trend/CLDTOT/'
cldtot_files = [
    base_path_cldtot + 'merged_CLDTOT_CTL_h0.nc',
    base_path_cldtot + 'merged_CLDTOT_AF50_h0.nc',
    base_path_cldtot + 'merged_CLDTOT_BE50_h0.nc',
    base_path_cldtot + 'merged_CLDTOT_REAL_h0.nc'
]
titles = [
    '(a) Annual CLDTOT in CTL',
    '(b) Annual CLDTOT in AF50',
    '(c) Annual CLDTOT in BE50',
    '(d) Annual CLDTOT in REAL'
]
```

```python
import xarray as xr
import matplotlib.pyplot as plt
import numpy as np
import scipy.stats as stats
import cmaps
import matplotlib.ticker as mticker
from matplotlib.colors import BoundaryNorm
from matplotlib.lines import Line2D
import matplotlib.patches as mpatches

# ====================== 1.
# ====================== 1. Trend calc ======================
def calculate_trends(data):
    years = np.arange(len(data))
    slope, intercept, r_value, p_value, std_err = stats.linregress(years, data)
    return slope, intercept, r_value, p_value

# ====================== 2. Bootstrap 95% CI ======================
def calc_bootstrap_ci(years, data, n_boot=1000, ci=95):
    x = np.arange(len(years))
    slope, intercept, _, _, _ = stats.linregress(x, data)
    fitted = intercept + slope * x
    resid = data - fitted

    boot_slopes = []
    boot_intercepts = []
    rng = np.random.default_rng()
    for _ in range(n_boot):
        boot_resid = rng.choice(resid, size=len(resid), replace=True)
        boot_y = fitted + boot_resid
        s, i, _, _, _ = stats.linregress(x, boot_y)
        boot_slopes.append(s)
        boot_intercepts.append(i)

    boot_slopes = np.array(boot_slopes)[:, np.newaxis]          # (n_boot, 1)
    boot_intercepts = np.array(boot_intercepts)[:, np.newaxis]  # (n_boot, 1)
    boot_trends = boot_slopes * x + boot_intercepts            # (n_boot, n_years)


    lower_line = np.percentile(boot_trends, (100 - ci) / 2, axis=0)
    upper_line = np.percentile(boot_trends, 100 - (100 - ci) / 2, axis=0)

    slope_lower = np.percentile(boot_slopes, (100 - ci) / 2)
    slope_upper = np.percentile(boot_slopes, 100 - (100 - ci) / 2)

    return lower_line, upper_line, slope_lower, slope_upper

# ====================== 3. File path ======================
base_path_cldtot = 'C:/JupyterXPC/Cloud_Analysis_AF_BE_Cloud_Trend/CLDTOT/'
cldtot_files = [
    base_path_cldtot + 'merged_CLDTOT_CTL_h0.nc',
    base_path_cldtot + 'merged_CLDTOT_AF50_h0.nc',
    base_path_cldtot + 'merged_CLDTOT_BE50_h0.nc',
    base_path_cldtot + 'merged_CLDTOT_REAL_h0.nc'
]
titles = [
    '(a) Annual CLDTOT in CTL',
    '(b) Annual CLDTOT in AF50',
    '(c) Annual CLDTOT in BE50',
    '(d) Annual CLDTOT in REAL'
]
```

NEW

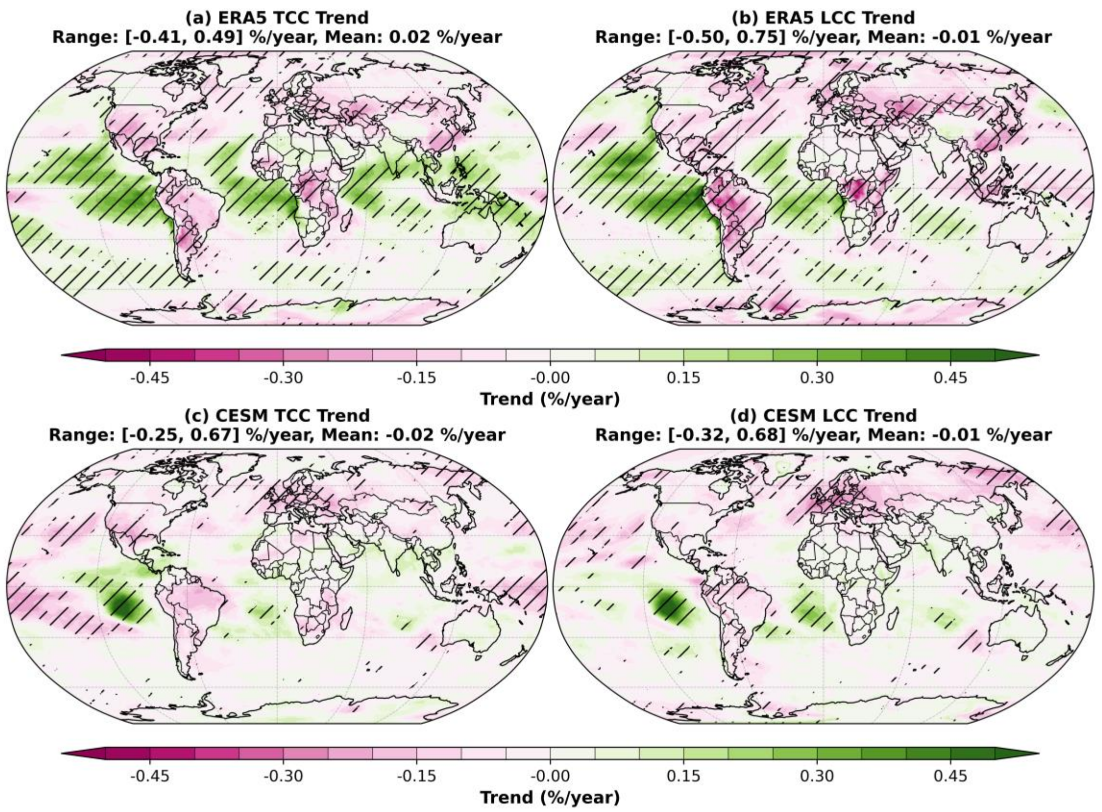

6.2. <u>Figure Presentation and Interpretability: Figs. 2, 3: The captions are currently quite brief and would greatly benefit from more detail to guide the reader. Please describe the panels more explicitly. For instance, are these long-term trends or Δvalues? If they are Δvalues, what is the reference run (e.g., CTL)? It would also be helpful to clarify what positive and negative values represent physically.</u>

We are very grateful for your valuable comments. Indeed, our current figure captions were overly brief, which might prevent readers from accurately understanding the meaning represented by each subplot. Therefore, in the revised manuscript, we have comprehensively rewritten and expanded these figure captions to ensure clarity of expression.

Regarding whether the presented results represent changes or absolute values, we explicitly define the control experiment (CTL) as the reference baseline run, and all difference values are calculated as sensitivity experiments (AF50, BE50, and REAL) minus the CTL experiment, as demonstrated in Equation 3 of the main text. However, in certain places, such as Fig. 1, we chose not to display difference values, particularly when presenting overall global trends, as expressing them as differences might instead impair clarity (because small difference values can be less intuitive and make comparing fold-changes less straightforward). On the contrary, directly showing the trend values within each experiment (including CTL) is more intuitive (for instance, in Fig. 1, the trend of low-level cloud cover in the CTL simulation is -0.0153±0.0030%/year, whereas in AF50 it is -0.0175±0.0036%/year, which very directly identifies that AF50 exacerbates the rate of low-level cloud loss). Furthermore, we have supplemented the color bar with clear physical interpretations, including the meanings of positive and negative values.

6.3. <u>Figure Presentation and Interpretability: Figure 6：The application of the Lorenz curve and the Gini coefficient to cloud trends is innovative, but the current presentation lacks physical context and can be misleading. By isolating positive (+) and negative (−) trends into separate panels that are normalized to 100% on the y-axis, the reader cannot tell which trend direction actually dominates the hemisphere. For instance, if a hemisphere is overwhelmingly dominated by cloud loss, a high Gini coefficient calculated for a smaller area showing a positive (+) cloud trend would be physically minor but visually overemphasized as being equally important. I strongly suggest adding a table or text annotations within each panel showing the relative area fraction or the integrated absolute magnitude of the (+) vs. (−) grid cells. Additionally, the monochromatic orange/blue continuous colormaps make it highly challenging to distinguish between the latitudinal bands referenced in the text. I suggest replacing these smooth gradients with a discrete, stepped colormap that clearly delineates distinct zones (e.g., separate color steps for Tropical, Mid-latitude, and Polar regions).</u>

We are very grateful for your highly insightful and constructive comment, and we also deeply appreciate your affirmation of our innovative application of the Lorenz curve and Gini index to cloud cover research. We believe that introducing this method allows for an intuitive evaluation of whether LUCC-induced cloud cover trends are broadly distributed in space or concentrated in a few latitudes. These two contrasting distributional directions are crucial for studying cloud cover trends, as it usually implies that if LUCC-induced cloud loss trends are concentrated in a few latitudinal bands (a Gini index closer to 1), the potential climatic and ecological consequences could be severe, much like recent research on precipitation concentration suggests—where Gini-index-based evaluations similarly demonstrated that regional precipitation concentration exacerbates droughts and terrestrial water storage deficits (Lesk and Mankin, 2026: Lesk, C. S., Mankin, J. S. More concentrated precipitation decreases terrestrial water storage. Nature 653, 425–432 (2026). https://doi.org/10.1038/s41586-026-10487-7). This offers important insights for our focus on cloud loss trends.

More importantly, we completely agree with your critique that normalizing both positive and negative trends to 100% without physical context visually overemphasizes secondary trends and could potentially mislead readers. Your suggestions for improvement are excellent, and we have adopted them in the revised figures. Specifically, we made the corresponding modifications: Adding physical context (grid cell area proportions of positive vs. negative cloud trends between hemispheres): To ensure readers can immediately discern the dominant trend direction within a hemisphere, we added clear text annotations to each subplot. These annotations display the relative grid-area proportions of positive (+) versus negative (−) grid cells, thereby placing the calculated Gini indices into proper physical perspective. Furthermore, regarding the display of the Gini index colorbar, we chose to adopt your valuable suggestion, as this approach has been utilized in recent research to provide a standard template and indeed employs a discrete colorbar for representation (Zhao et al., 2025: Haipeng Zhao et al., Greener green and bluer blue: Ocean poleward greening over the past two decades. Science 388, 1337–1340 (2025). DOI: 10.1126/science.adr9715).

Greenland and Antarctica because of the dominant influence of their ice caps.

Fig. 1: Trends and variability in TWS and rainfall concentration.

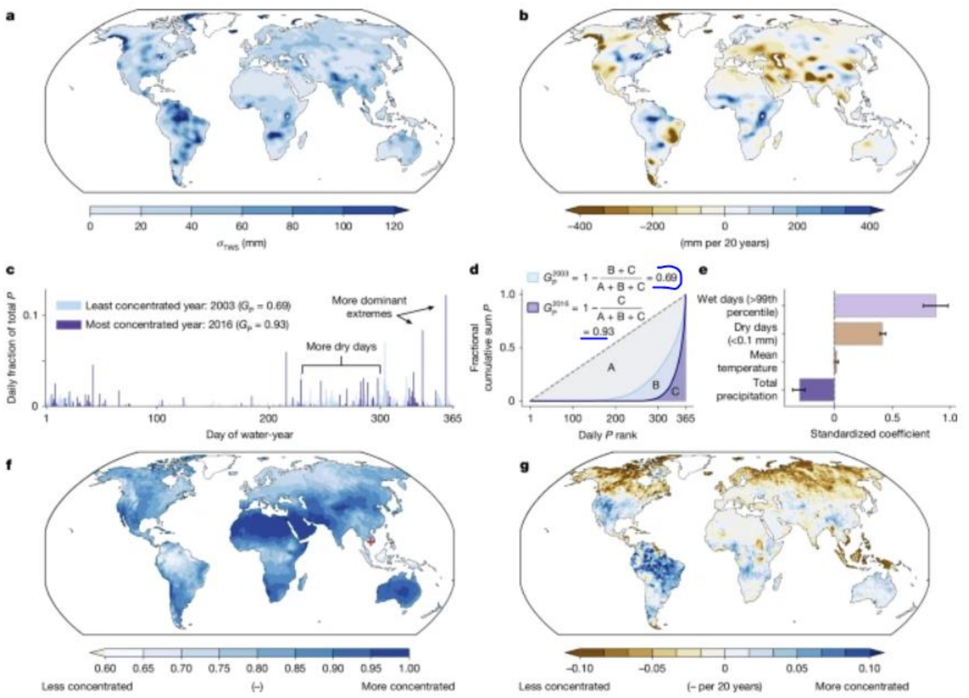

limits phytoplankton biomass (18) in the high nutrient–low chlorophyll Southern Ocean.

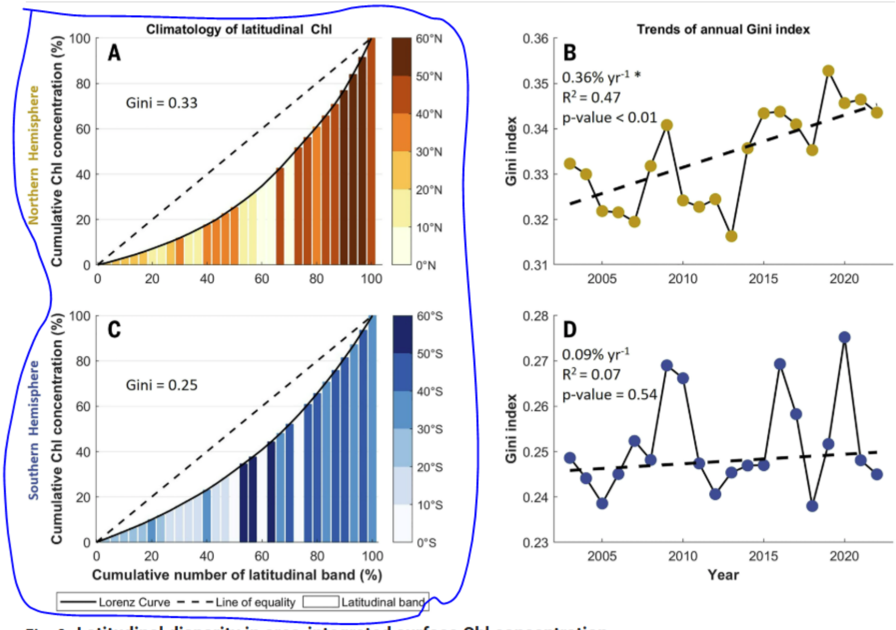

Fig. 2. **Latitudinal disparity in area-integrated surface Chl concentration.**
(**A** and **C**) Lorenz curves of climatological Chl area-integrated over 2° latitudinal bands in the Northern (0° to 60°N) and Southern Hemispheres (0° to 60°S) during the 2003–2022 period. Bars represent the cumulative percentage of surface Chl integrated over 2° latitudinal bands, ordered in ascending contribution of Chl to the total. (**B** and **D**) Interannual variability of the Gini index from 2003 to 2022, with significant trends (*P* < 0.05) indicated by an asterisk.

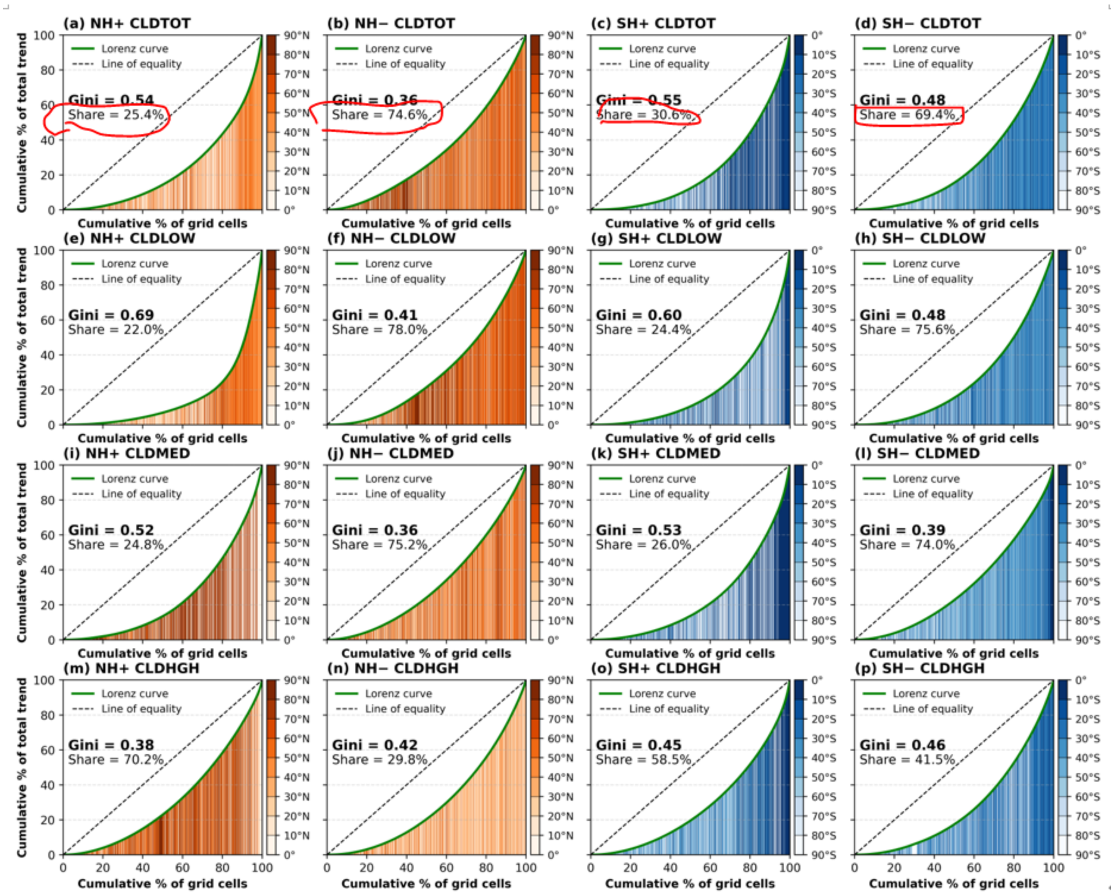

6.4. **<u>Figure Presentation and Interpretability: Figure 7, SHAP Analysis: The use of SHAP values needs to be more accessible. Please explain the intuition of the color bar ("Feature value: High vs. Low") in relation to the x-axis (SHAP value) in the text or caption. Furthermore, the inset bar charts in Fig. 7 are currently too small and unreadable. To save space, panels sharing variables (a, b, c) should share a single y-axis and color bar, allowing the insets to be enlarged or moved to the supplement. Finally, please state in the caption if the features on the y-axis are ranked by overall importance.</u>**

We are very grateful for your suggestions regarding the improvement of figure readability. Indeed, the SHAP plot (Fig. 7) in the original manuscript appeared somewhat crowded, and the embedded bar charts were difficult to read, making them legible only upon zooming in on the page; please forgive our oversight in this regard. To enhance the readability and interpretability of the figure, we have completely reorganized Fig. 7. Specifically, we removed the inset bar charts representing contributions from the original Fig. 7 and relocated them to Fig. 8 for clear display. Furthermore, to make the SHAP analysis more accessible and easier to understand, we added explicit explanations in the figure caption. We clarified the relationship between the color bar (feature value level) and the x-axis: the color bar indicates high versus low feature values, where feature values refer to the long-term trend of the difference between each sensitivity experiment and the control experiment. Because our modeling targets LUCC-induced cloud cover trends, the names of the drivers on the y-axis of the SHAP plot are preceded by the difference symbol (Δ).It should also be noted that these variables were already ranked by feature importance—a point we did not explain in the earlier version, but in the revised manuscript, we explicitly specify that the SHAP plot is sorted by feature importance. When purple (high feature value) is distributed along the positive x-axis, it indicates that a LUCC-induced increase in this climate feature drives an increase in the predicted cloud cover trend (i.e., making a positive contribution), consistent with standard SHAP visualizations in most studies (

1.Andrea K. Tokranov et al. ,Predictions of groundwater PFAS occurrence at drinking water supply depths in the United States. Science. 386,748-755(2024).DOI:10.1126/science.ado6638;

2. M. Berdugo, J. J. Gaitán, M. Delgado-Baquerizo, T. W. Crowther, V. Dakos, Prevalence and drivers of abrupt vegetation shifts in global drylands. Proc. Natl. Acad. Sci. U.S.A. 119, e2123393119 (2022);

3. Wang, Y., Liu, D., Wang, H., Shi, S., Hu, Q., Wang, Z., Liu, Z., Zhao, T., and Shen, L.: Synchronization of source and sink by boundary layer evolution: a key to new particle formation under varying ozone pollution, Atmos. Chem. Phys., 26, 7827–7842, https://doi.org/10.5194/acp-26-7827-2026, 2026.).

ance reduction. However, both variables are important to the model, indicating that population density provides additional information to the model that further reduces variance. This is also the case for other correlated variables in the final model (fig. S13).

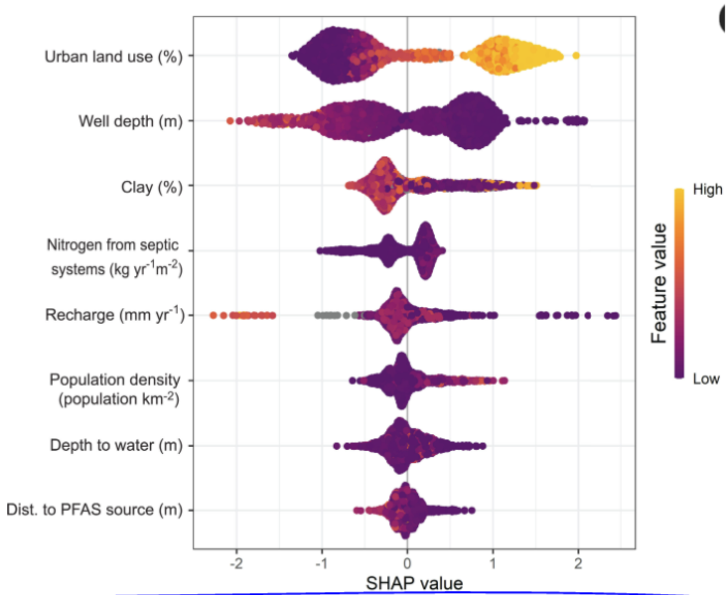

Fig. 3. SHAP plot for model training data for detection of PFAS.
Variables are organized from most to least important (fig. S11) from top to bottom of the figure. Positive SHAP values correspond to an increased probability of detection and vice versa (SHAP value units are in log odds). SHAP values are computed relative to the average prediction, indicated as zero on the *x* axis. Colors on the SHAP plot range from low (purple) to high (yellow) values of the predictor variable. Missing values are shown in gray.

seasonality on ecosystem productivity (30), e.g., monsoonal climates in India (31).

Fig. 2.

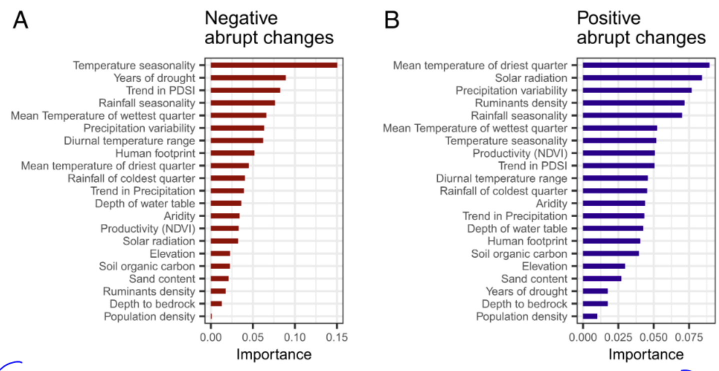

Drivers of abrupt changes have contrasting importance depending on the trend of NDVI analyzed. Ranked importance for negative (A) and positive (B) abrupt changes. Importance is measured as gain and represents the improvement in accuracy of the RF model when a factor is included. The model fitted is a RF algorithm confronting abruptness (1 if abrupt, 0 otherwise) with 21 uncorrelated environmental factors summarizing climatic, soil, topographical, and human-related drivers. Total number of instances used to train/validate the model is 1955/839 for negative abrupt changes and 9135/3915 for positive abrupt changes.

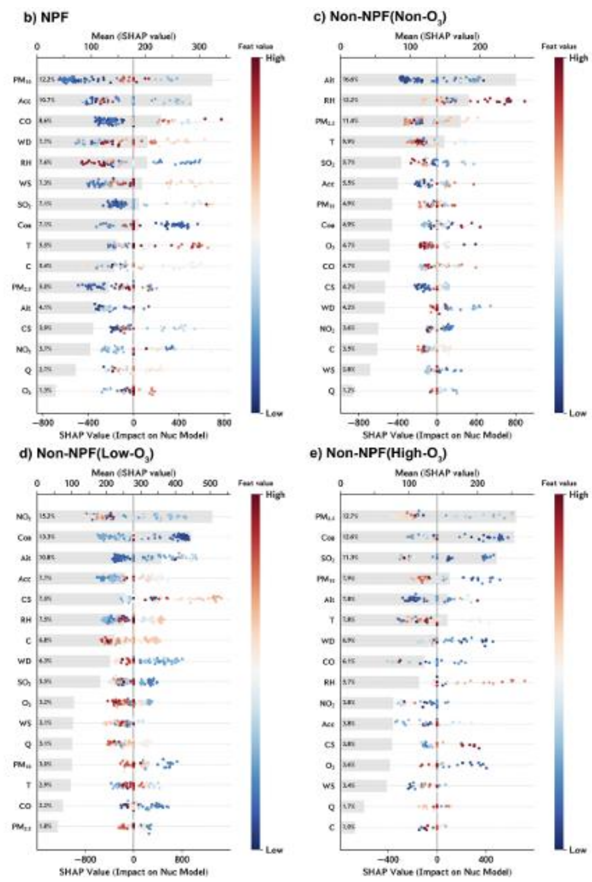

Figure 6. SHAP-based analysis of drivers for particle number concentrations in the Nuc mode. **(a)** Mean SHAP values across the four scenarios, with red, yellow, blue, and black bars represent the NPF, Non-NPF (Non-O_3), Non-NPF (Low-O_3) and Non-NPF (High-O_3) scenarios, respectively. **(b–e)** Feature importance and summary plots for **(b)** NPF, **(c)** Non-NPF (Non-O_3), **(d)** Non-NPF (Low-O_3), **(e)** Non-NPF (High-O_3) scenario. The bar charts indicate the mean absolute SHAP values, while the scatter plots show the distribution of SHAP values, with colors transitioning from blue (low feature values) to red (high feature values).

 https://doi.org/10.5194/acp-26-7827-2026

Specific comments

7. <u>Title：The title in the preprint contains a typo (“amplifiers”) and does not match the corrected title in the online EGUsphere version.</u>

We are very grateful for your thorough check. Regarding this issue present in the title, we have corrected it in the revised manuscript, and the corrected result is also displayed in the preprint following the EGU technical check. In the original version, the word "amplifiers" contained an extra letter "r"; we have removed the letter "r" in the revised version. We once again express our most sincere gratitude for your valuable time and meticulous review.

8. <u>Abstract：The relative numbers provided are unclear. Relative to what baseline?</u>

We are very grateful for your valuable feedback. Indeed, in the current version, we failed to clearly explain the relevant numerical values. In fact, when presenting differences, all of our data are calculated relative to the control experiment, that is, the sensitivity experiment minus the control experiment. To address this issue, we have thoroughly re-examined the numbers mentioned in the Abstract and revised the text to ensure clearer expression.

9. <u>Acronyms & Variables：The paper has a lot of acronyms, making it difficult to read. I suggest using far fewer acronyms and wherever possible use conventional acronyms some readers might already be familiar with.</u>

We sincerely thank you for pointing out this issue. We completely agree that the excessive use of abbreviations in the previous version (e.g., FAO, CESM, AF50, BE50, REAL, CLDTOT, CLDLOW, CLDMED, CLDHGH, etc.) could easily disrupt the reading flow, making the manuscript difficult to follow. In response to your valuable feedback, we have thoroughly reviewed and revised the main text to minimize the use of abbreviations, thereby enhancing overall readability.

However, certain abbreviations are necessary to retain—such as CESM, as well as the names of each experiment (CTL, AF50, BE50, and REAL)—though we have ensured that their full names are explicitly defined upon their first occurrence. Similarly, we needed to retain standard output variable names from the CESM model, such as cloud cover variables (CLDTOT, CLDLOW, CLDMED, and CLDHGH) and related climate factors. Other abbreviations were also preserved, such as SHAP and XGBoost, as this conforms to standard practice in numerous studies and maintains the conciseness of proper technical terminology.

10. <u>The term "bioenergy": currently reads a bit like jargon and would benefit from a brief functional explanation. I recommend adding a short definition around Line 93 in the introduction, and perhaps including a few clarifying words in the abstract as well to ensure it is clear to all readers.</u>

We thank you for your valuable comment. We agree that the term "bioenergy" might be perceived as jargon by a broader audience, and thus providing a clear functional explanation is necessary to significantly enhance the readability of the paper. Therefore, following your suggestion, we have added clarifying definitions in both the Abstract and the Introduction—specifically noting that bioenergy refers to the large-scale cultivation of dedicated energy crops for renewable electricity generation or biofuel production, the widespread deployment of which represents a major driver of future land-use and land-cover change. Indeed, while we had detailed this land-use change pathway involving bioenergy crops in the experimental design section, we fully agree that presenting it clearly in the Abstract is beneficial.

11. <u>Line 171: The first reference to a Supplementary Information (SI) figure jumps to Figs. S24–S27. Might be better to reorder the SI figures so they appear sequentially as mentioned in the main text.</u>

We thank you for your valuable comment. Indeed, our previous manuscript failed to account for the alignment between the supplementary figures and the narrative in the main text, resulting in substantial jumps that disrupted reading continuity. We are very grateful for your insightful feedback. To address this issue, we have reordered the figures in the Supplementary Information to strictly follow the sequence in which they are cited in the main text.

12. <u>Line 180:   "landuse.timeseries" – Typo?</u>

We thank you for your valuable comment. The term "landuse.timeseries" is not a typo. Therefore, we have retained this usage in the main text, as this expression intuitively reflects that our simulations are transient simulations, that is, the land-use forcing varies on an annual basis over time. This usage has also been adopted in previous studies (e.g., Cheng et al., 2022: Future bioenergy expansion could alter carbon sequestration potential and exacerbate water stress in the United States. Sci. Adv. 8, eabm8237 (2022). DOI: 10.1126/sciadv.abm8237). On the other hand, this phrasing also corresponds to the official naming convention of CESM input data (https://svn-ccsm-inputdata.cgd.ucar.edu/trunk/inputdata/lnd/clm2/surfdata_map/), which we speculate was intended by the official repository to highlight that the land-cover dataset is dynamic and time-evolving.

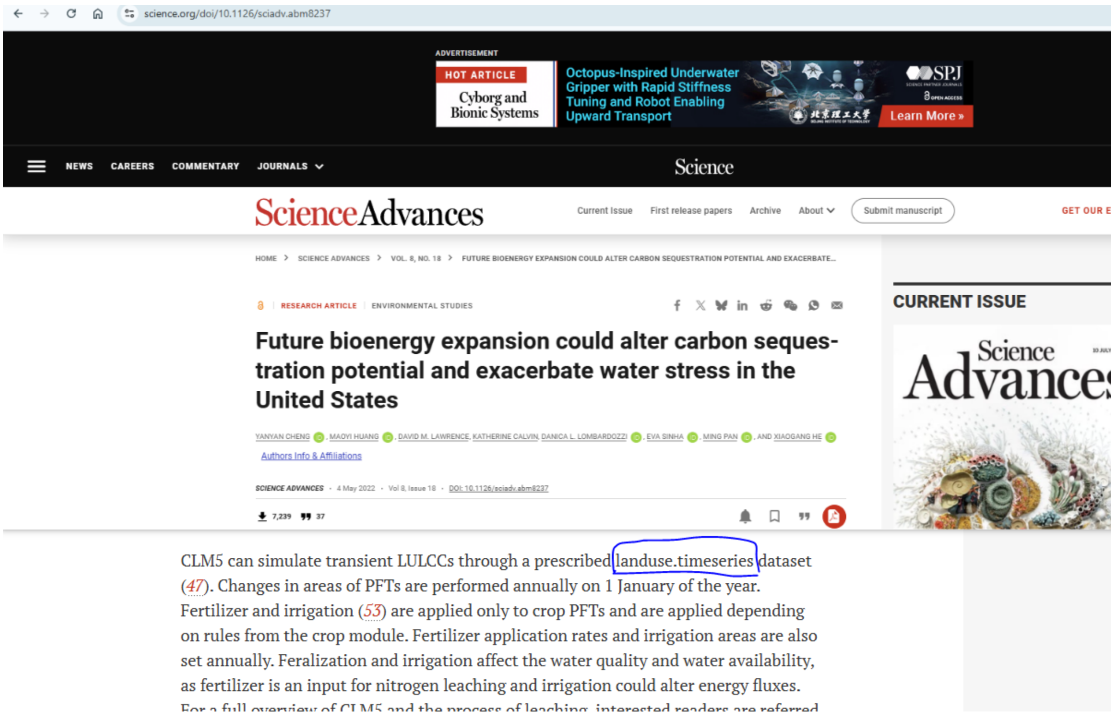
science.org/doi/10.1126/sciadv.abm8237

ADVERTISEMENT

HOT ARTICLE

Cyborg and Bionic Systems

Octopus-Inspired Underwater Gripper with Rapid Stiffness Tuning and Robot Enabling Upward Transport

SPJ

Learn More »

NEWS CAREERS COMMENTARY JOURNALS

Science

ScienceAdvances

Current Issue First release papers Archive About Submit manuscript GET OUR E

HOME > SCIENCE ADVANCES > VOL. 8, NO. 18 > FUTURE BIOENERGY EXPANSION COULD ALTER CARBON SEQUESTRATION POTENTIAL AND EXACERBATE...

RESEARCH ARTICLE | ENVIRONMENTAL STUDIES

Future bioenergy expansion could alter carbon sequestration potential and exacerbate water stress in the United States

YANYAN CHENG, MAOYI HUANG, DAVID M. LAWRENCE, KATHERINE CALVIN, DANICA L. LOMBARDOZZI, EVA SINHA, MING PAN, AND XIAOGANG HE

Authors Info & Affiliations

SCIENCE ADVANCES • 4 May 2022 • Vol 8, Issue 18 • DOI: 10.1126/sciadv.abm8237

7,239 37

CURRENT ISSUE

Science Advances

CLM5 can simulate transient LULCCs through a prescribed landuse.timeseries dataset (47). Changes in areas of PFTs are performed annually on 1 January of the year. Fertilizer and irrigation (53) are applied only to crop PFTs and are applied depending on rules from the crop module. Fertilizer application rates and irrigation areas are also set annually. Feralization and irrigation affect the water quality and water availability, as fertilizer is an input for nitrogen leaching and irrigation could alter energy fluxes.

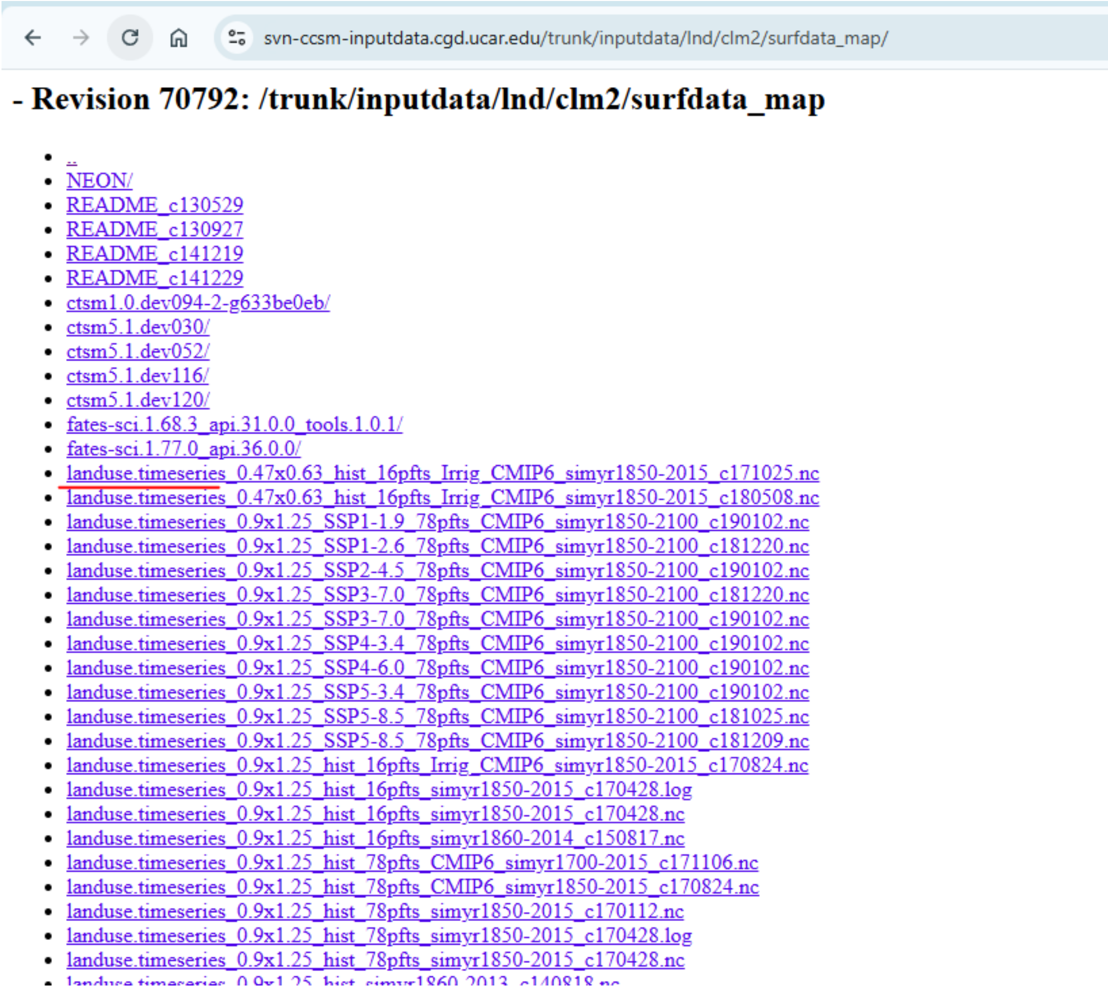

svn-ccsm-inputdata.cgd.ucar.edu/trunk/inputdata/lnd/clm2/surfdata_map/

- Revision 70792: /trunk/inputdata/lnd/clm2/surfdata_map

- ..
- NEON/
- README_c130529
- README_c130927
- README_c141219
- README_c141229
- ctsm1.0.dev094-2-g633be0eb/
- ctsm5.1.dev030/
- ctsm5.1.dev052/
- ctsm5.1.dev116/
- ctsm5.1.dev120/
- fates-sci.1.68.3_api.31.0.0_tools.1.0.1/
- fates-sci.1.77.0_api.36.0.0/
- landuse.timeseries_0.47x0.63_hist_16pfts_Irrig_CMIP6_simyr1850-2015_c171025.nc
- landuse.timeseries_0.47x0.63_hist_16pfts_Irrig_CMIP6_simyr1850-2015_c180508.nc
- landuse.timeseries_0.9x1.25_SSP1-1.9_78pfts_CMIP6_simyr1850-2100_c190102.nc
- landuse.timeseries_0.9x1.25_SSP1-2.6_78pfts_CMIP6_simyr1850-2100_c181220.nc
- landuse.timeseries_0.9x1.25_SSP2-4.5_78pfts_CMIP6_simyr1850-2100_c190102.nc
- landuse.timeseries_0.9x1.25_SSP3-7.0_78pfts_CMIP6_simyr1850-2100_c181220.nc
- landuse.timeseries_0.9x1.25_SSP3-7.0_78pfts_CMIP6_simyr1850-2100_c190102.nc
- landuse.timeseries_0.9x1.25_SSP4-3.4_78pfts_CMIP6_simyr1850-2100_c190102.nc
- landuse.timeseries_0.9x1.25_SSP4-6.0_78pfts_CMIP6_simyr1850-2100_c190102.nc
- landuse.timeseries_0.9x1.25_SSP5-3.4_78pfts_CMIP6_simyr1850-2100_c190102.nc
- landuse.timeseries_0.9x1.25_SSP5-8.5_78pfts_CMIP6_simyr1850-2100_c181025.nc
- landuse.timeseries_0.9x1.25_SSP5-8.5_78pfts_CMIP6_simyr1850-2100_c181209.nc
- landuse.timeseries_0.9x1.25_hist_16pfts_Irrig_CMIP6_simyr1850-2015_c170824.nc
- landuse.timeseries_0.9x1.25_hist_16pfts_simyr1850-2015_c170428.log
- landuse.timeseries_0.9x1.25_hist_16pfts_simyr1850-2015_c170428.nc
- landuse.timeseries_0.9x1.25_hist_16pfts_simyr1860-2014_c150817.nc
- landuse.timeseries_0.9x1.25_hist_78pfts_CMIP6_simyr1700-2015_c171106.nc
- landuse.timeseries_0.9x1.25_hist_78pfts_CMIP6_simyr1850-2015_c170824.nc
- landuse.timeseries_0.9x1.25_hist_78pfts_simyr1850-2015_c170112.nc
- landuse.timeseries_0.9x1.25_hist_78pfts_simyr1850-2015_c170428.log
- landuse.timeseries_0.9x1.25_hist_78pfts_simyr1850-2015_c170428.nc

13. <u>Line 183: "FAO" appears here for the first time but is not defined until Line 603. Please ensure it is defined upon its first use in the text.</u>

We are very grateful for your valuable comment. Please forgive our oversight in failing to explicitly define the abbreviation FAO upon its first occurrence. In the revised manuscript, we have corrected this issue by spelling out its full name: the Food and Agriculture Organization of the United Nations (FAO). This organization defines not only the concept of forests but also that of afforestation (https://openknowledge.fao.org/server/api/core/bitstreams/531a9e1b-596d-4b07-b9fd-3103fb4d0e72/content). Furthermore, we have conducted a full audit of all abbreviations upon their first appearance throughout the manuscript to ensure that similar issues are avoided.

OTHER PLANTED FOREST

<u>Planted forest</u> which is not classified as <u>plantation forest</u>.

1c ANNUAL FOREST EXPANSION, DEFORESTATION AND NET CHANGE

FOREST EXPANSION

Expansion of <u>forest</u> on land that, until then, was under a different land use, implies a transformation of land use from non-forest to forest.

AFFORESTATION (Sub-category of FOREST EXPANSION)

Establishment of <u>forest</u> through planting and/or deliberate seeding on land that, until then, was under a different land use, implies a transformation of land use form non-forest to forest.

NATURAL EXPANSION OF FOREST (Sub-category of FOREST EXPANSION)

Expansion of <u>forest</u> through natural succession on land that, until then, was under a different land use, implies a transformation of land use form non-forest to forest (e.g. forest succession on land previously used for agriculture).

DEFORESTATION

The conversion of <u>forest</u> to other land use independently whether human-induced or not.

Explanatory notes

1. Includes permanent reduction of the <u>tree canopy cover</u> below the minimum 10 percent threshold.
2. It includes areas of forest converted to agriculture, pasture, water reservoirs, mining and urban areas.
3. The term specifically excludes areas where the trees have been removed as a result of harvesting or logging, and where the forest is expected to regenerate naturally or with the aid of silvicultural measures.
4. The term also includes areas where, for example, the impact of disturbance, over-utilization or changing environmental conditions affects the forest to an extent that it cannot sustain a canopy cover above the 10 percent threshold.

14. <u>Line 230+： Please include units for all variables discussed in the text, including those related to Equation 6.</u>

We sincerely thank you for pointing out this oversight. We have carefully checked the entire manuscript and added standard units for all physical variables in the text, almost all of which are derived from the default units in CESM (e.g., the unit for sensible heat flux is W/m^2). For dimensionless variables or ratios, we have also explicitly stated that they are dimensionless. We believe these additions will significantly enhance the clarity and rigor of our methodology.

15. <u>Line 301： There appears to be a typo in the error bounds: "-0.0083 ± 1037%/year". Additionally, it would be much more intuitive to present these trends per decade rather than per year.</u>

We sincerely thank you for taking the valuable time to conduct such a rigorous review of our study, which has truly reinforced the importance of maintaining scientific rigor in our future work. Please forgive our oversight during manuscript preparation. In addition, we have corrected the code used for calculating confidence intervals, as detailed in our response to Comment 6.1. Regarding the presentation of trends, we have opted to retain our current approach of reporting annual trends rather than decadal trends. Expressing trends on an annual basis is a well-established convention in previous literature (e.g., Luo et al., 2024: Diurnally asymmetric cloud cover trends amplify greenhouse warming. Sci. Adv. 10, eado5179 (2024). DOI: 10.1126/sciadv.ado5179). We believe annual rates are more intuitive and tangible to interpret than decadal scales, which can feel somewhat abstract. Furthermore, because the land-use forcing dataset varies on an annual basis, presenting the simulated cloud cover and associated atmospheric response trends on an annual timescale provides a more consistent alignment with the underlying forcing.

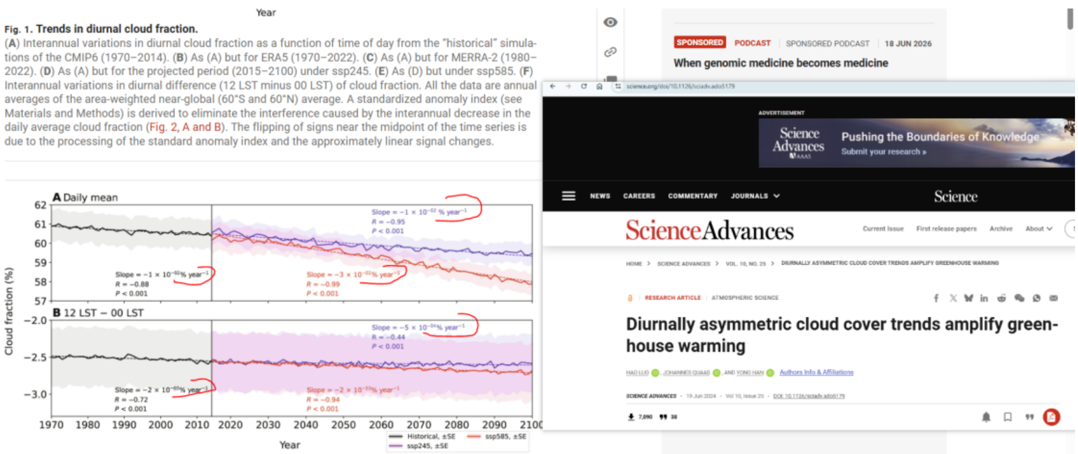

16. <u>Lines 364 & 373: I suggest avoiding subjective phrases like "climate damage" or "negative impacts on the climate." Maintain scientific descriptive, objective scientific language (e.g., "amplified warming").</u>

We are deeply grateful for your valuable comment. Indeed, we should avoid overly subjective language; maintaining objective and strictly descriptive scientific language is essential for this manuscript. In the revised version, we thoroughly audited the entire text to eliminate any subjective or value-laden phrasing. We once again express our most sincere gratitude for the valuable time and effort you have invested. These insightful comments have not only improved the present study, but more importantly, will guide us to consciously maintain an objective description of research findings in our future work.

17. <u>Lines 493–497：The “Mesosphere clouds” – is this a terminology error? The authors discuss the loss of “mesosphere clouds” due to boundary layer changes suppressing moisture supply. The CESM variable CLDHGH represents upper tropospheric clouds. Please clarify.</u>

We are very grateful for your rigorous review. Fortunately, your thorough check helped us identify and correct this scientific inaccuracy, and we have fully addressed this issue in the revised manuscript.

18. <u>Lines 596–597：The phrasing “the land comes from the land of other bioenergy crops” is awkward and should be rewritten for clarity.</u>

We are very grateful for your valuable comment. Regarding this sentence, what we intended to convey is that the land utilized for bioenergy crop expansion in our simulations is converted from other crop lands, which differs from idealized afforestation (where land is derived from grasslands or shrublands). In fact, this point is closely related to your first comment. In CLM5, sugarcane is explicitly categorized into rainfed sugarcane and irrigated sugarcane, corresponding to indices 67 and 68, respectively. Meanwhile, Index 0 represents bare ground; indices 1 – 8 represent tree types; and indices 9 – 14 represent shrubs and grasses, which serve as the source lands for forest expansion in our study. This mode of forest expansion strictly adheres to the FAO definition of afforestation. In the bioenergy crop expansion experiment, the land area required for sugarcane expansion (both rainfed and irrigated) is reallocated from other crop lands. As demonstrated in existing repositories (https://github.com/AnushaNTNU/BetZy-scripts/blob/main/compare_modifiedvsoriginal_landuse.ipynb), bioenergy crop expansion operates as a zero-sum trade-off to ensure area conservation. Similarly, in idealized afforestation, deriving land from grasslands or shrublands is likewise designed to preserve total land area, fulfilling CESM's strict requirement that patch-level land-cover alterations must sum to 100% at the grid-cell level.

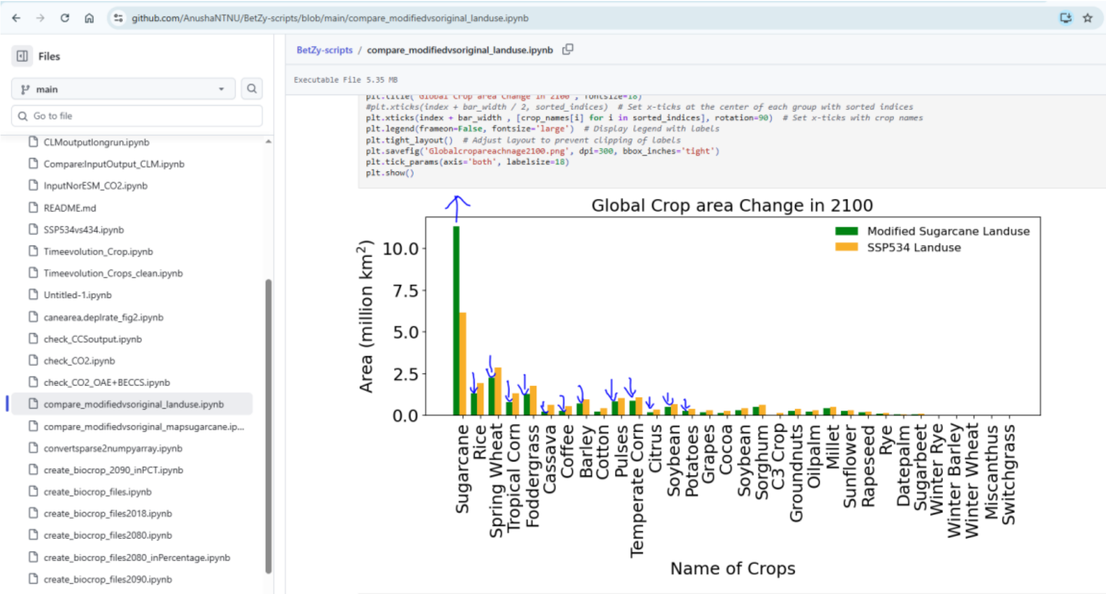

Finally, we would like to take this opportunity to express our sincere gratitude to the editor and reviewers of Atmospheric Chemistry and Physics (ACP) for their valuable time, effort, and highly constructive feedback in improving our work. Without a doubt, these comments have significantly enhanced the objectivity, scientific rigor, and linguistic precision of our manuscript, as well as the overall clarity of our figures. Furthermore, it has been a privilege to engage in this meaningful scientific dialogue with the reviewers, which has further stimulated our research interest in the climate and ecological consequences of large-scale land-use change, particularly afforestation practices, which are currently, and will likely continue to be, widely pursued. We must emphasize that evaluating the potential climate consequences of highly favored afforestation efforts necessitates taking cloud feedback processes into account (for instance, in our simulations, even realistic afforestation induced a significant increasing trend in high-level clouds, which exert positive radiative forcing and can induce a top-of-atmosphere energy imbalance; conversely, an increasing trend in low-level cloud cover might lead to the overly optimistic belief that realistic afforestation consistently yields cooling), just as previous studies have highlighted the equal importance of accounting for surface albedo.